

Article

Pd₂Spermine Complex Shows Cancer Selectivity and Efficacy to Inhibit Growth of Triple-Negative Breast Tumors in Mice

Martin Vojtek ^{1,*}, Salomé Gonçalves-Monteiro ¹, Patrícia Šeminská ¹, Katarína Valová ¹, Loreto Bellón ¹, Patrícia Dias-Pereira ², Franklim Marques ³, Maria P. M. Marques ^{4,5}, Ana L. M. Batista de Carvalho ⁴, Helder Mota-Filipe ⁶, Isabel M. P. L. V. O. Ferreira ⁷ and Carmen Diniz ^{1,*}

- ¹ LAQV/REQUIMTE, Laboratory of Pharmacology, Department of Drug Sciences, Faculty of Pharmacy, University of Porto, 4050-313 Porto, Portugal; salomemonteiro8180@gmail.com (S.G.-M.); patka.seminska@gmail.com (P.Š.); katusa.valova@gmail.com (K.V.); loreto.bellon@hotmail.com (L.B.)
- ² ICBAS—Instituto de Ciências Biomédicas de Abel Salazar, University of Porto, 4050-313 Porto, Portugal; pdpereira@icbas.up.pt
- ³ Clinical Analysis Unit, Faculty of Pharmacy, University of Porto, 4050-313 Porto, Portugal; franklim@ff.up.pt
- ⁴ “Molecular Physical-Chemistry” R&D Unit, Department of Chemistry, University of Coimbra, 3004-535 Coimbra, Portugal; pmc@ci.uc.pt (M.P.M.M.); almbc@uc.pt (A.L.M.B.d.C.)
- ⁵ Department of Life Sciences, University of Coimbra, 3000-456 Coimbra, Portugal
- ⁶ iMed.Ulisboa, Faculty of Pharmacy, University of Lisbon, 1649-003 Lisbon, Portugal; hfilipe@campus.ul.pt
- ⁷ LAQV/REQUIMTE, Laboratory of Bromatology and Hydrology, Department of Chemical Sciences, Faculty of Pharmacy, University of Porto, 4050-313 Porto, Portugal; isabel.ferreira@ff.up.pt
- * Correspondence: matovoj@gmail.com (M.V.); cdiniz@ff.up.pt (C.D.)



Citation: Vojtek, M.; Gonçalves-Monteiro, S.; Šeminská, P.; Valová, K.; Bellón, L.; Dias-Pereira, P.; Marques, F.; Marques, M.P.M.; Batista de Carvalho, A.L.M.; Mota-Filipe, H.; et al. Pd₂Spermine Complex Shows Cancer Selectivity and Efficacy to Inhibit Growth of Triple-Negative Breast Tumors in Mice. *Biomedicines* **2022**, *10*, 210. <https://doi.org/10.3390/biomedicines10020210>

Academic Editors: Muhammad Hanif and Tania Gamberi

Received: 9 December 2021

Accepted: 14 January 2022

Published: 19 January 2022

Publisher’s Note: MDPI stays neutral with regard to jurisdictional claims in published maps and institutional affiliations.



Copyright: © 2022 by the authors. Licensee MDPI, Basel, Switzerland. This article is an open access article distributed under the terms and conditions of the Creative Commons Attribution (CC BY) license (<https://creativecommons.org/licenses/by/4.0/>).

Abstract: Pd₂Spm is a dinuclear palladium(II)-spermine chelate with promising anticancer properties against triple-negative breast cancer (TNBC), a breast carcinoma subset with poor prognosis and limited treatment options. The present study evaluated the in vitro and in vivo anticancer effects of Pd₂Spm compared to the reference metal-based drug cisplatin. Triple-negative breast cancer MDA-MB-231 cells, non-cancerous MCF-12A breast cells and chorioallantoic membrane (CAM) assay were used for antiproliferative, antimigratory and antiangiogenic studies. For an in vivo efficacy study, female CBA nude mice with subcutaneously implanted MDA-MB-231 breast tumors were treated with Pd₂Spm (5 mg/kg/day) or cisplatin (2 mg/kg/day) administered intraperitoneally during 5 consecutive days. Promising selective antiproliferative activity of Pd₂Spm was observed in MDA-MB-231 cells (IC₅₀ values of 7.3–8.3 μM), with at least 10-fold lower activity in MCF-12A cells (IC₅₀ values of 89.5–228.9 μM). Pd₂Spm inhibited the migration of MDA-MB-231 cells, suppressed angiogenesis in CAM and decreased VEGF secretion from MDA-MB-231 cells with similar potency as cisplatin. Pd₂Spm-treated mice showed a significant reduction in tumor growth progression, and tumors evidenced a reduction in the Ki-67 proliferation index and number of mitotic figures, as well as increased DNA damage, similar to cisplatin-treated animals. Encouragingly, systemic toxicity (hematotoxicity and weight loss) observed in cisplatin-treated animals was not observed in Pd₂Spm-treated mice. The present study reports, for the first time, promising cancer selectivity, in vivo antitumor activity towards TNBC and a low systemic toxicity of Pd₂Spm. Thus, this agent may be viewed as a promising Pd(II) drug candidate for the treatment of this type of low-prognosis neoplasia.

Keywords: Pd(II)-based drugs; cisplatin; metal complexes; triple-negative breast cancer; in vivo; xenografts

1. Introduction

Female breast cancer is currently the most commonly diagnosed cancer and the leading type of cancer death in women worldwide, with 2.3 million new cases having been diagnosed in 2020 [1]. Breast cancer is a highly heterogeneous disease that presents several subtypes with different treatment success and survival prognosis. Triple-negative

breast cancer (TNBC) stands out as the most aggressive breast cancer subtype, constituting 10–30% of all breast cancer cases. TNBC is characterized by the absence of estrogen receptor and progesterone receptor, as well as HER2 overexpression, and disproportionately affects women with African or Indian ancestry, who show higher incidence of TNBC compared to other breast cancer subtypes [2]. TNBC is also associated with poorer prognosis than other subtypes of breast cancer, mainly due to higher frequency of metastasis, higher relapse rates and limited treatment options, with no conventional receptor-targeting therapeutics available compared to other breast cancer subtypes. However, owing to recent advances in the understanding of the distinctive biology and molecular features of TNBC, the TNBC therapeutic landscape of targeted therapies has been expanded with PARP inhibitors, antibody–drug conjugates and immune checkpoint inhibitors [3]. Nevertheless, platinum(II) chemotherapeutics such as cisplatin and carboplatin still remain the reference treatment of TNBC, either in adjuvant or neoadjuvant settings, and as monotherapy or in combination with other drugs [4,5]. Platinum-based chemotherapeutics are able to increase the disease-free survival time, but the overall survival of patients remains unchanged mainly due to the poor tolerability of the patients (resulting in dose reduction, yielding inferior clinical outcomes) and/or the development of tumor resistance over the treatment time course [4,5]. The most frequent unintended outcomes of platinum-based therapy are related to myelosuppression, gastrointestinal reactions and damage of liver and kidney functions, which may be mitigated to certain level by the pre-hydration of patients and other supporting measures [6].

Palladium-based compounds are being considered as promising analogs to platinum chemotherapeutics, owing to the similarities in structure and coordination chemistry between platinum and palladium ions. In particular, palladium complexes with aliphatic biogenic polyamines have been studied during the last decade, showing promising *in vitro* antiproliferative activity against several cancer types, including TNBC [7]. A dinuclear palladium complex with spermine (Pd_2Spm) is a particularly promising agent, with its *in vitro* antiproliferative activity already reported against various cancer types, including osteosarcoma [8], hormone-dependent breast carcinoma [9], ovarian cancer [10] and TNBC [11]. The pharmacological mechanism of action of Pd_2Spm is believed to be similar to cisplatin, with both being able to produce drug–DNA crosslinks that lead to cellular death. However, polyamine polynuclear complexes such as Pd_2Spm have been shown to produce distinctive long-range drug–DNA crosslinks, which are not observed for cisplatin and other classical platinum-based drugs and can prompt more severe and less-repairable DNA damage [12–14]. TNBC cells such as MDA-MB-231 cells demonstrated similar antiproliferative effects of Pd_2Spm and cisplatin [11], but it was reported that breast cancer cells accumulate approximately four times lower amounts of Pd_2Spm than cisplatin, i.e., a lower intracellular quantity of Pd_2Spm is required to produce similar antiproliferative effects. This implies the occurrence of alternative (yet unknown) anticancer molecular target(s) for Pd_2Spm versus cisplatin [15–18]. A recent pharmacokinetic study in mice also showed that while Pd_2Spm has a very similar serum terminal half-life to cisplatin, it presents a lower accumulation in major organs as compared to cisplatin [15]. Therefore, Pd_2Spm is expected to show a superior tolerability as well as lower nephrotoxicity/hepatotoxicity than cisplatin, owing to both lower tissue accumulation and decreased metabolic reactivity with kidney and liver biomolecules responsible for the associated toxicity (which was recently reported by our group) [15,19]. Based on these previous findings, the present study has sought to investigate, for the first time, the *in vivo* efficacy (to reduce tumor growth) and tolerability (changes in body weight, behavior, histopathological features and biochemical and hematological parameters) of a 5-day Pd_2Spm treatment compared to cisplatin's treatment in mice bearing TNBC MDA-MB-231 breast tumors. Additionally, the Pd_2Spm 's cancer selectivity was also assessed *in vitro*, along with the effects of Pd_2Spm on angiogenesis and MDA-MB-231 cell migration, to further broaden our understanding of this chelate.

2. Materials and Methods

2.1. Reagents and Chemicals

Cisplatin (*cis*-dichlorodiammine platinum(II), 99.9%), potassium tetrachloropalladate (II) (K_2PdCl_4 , 98%), spermine (N,N'-bis(3-aminopropyl)-1,4-diaminobutane, 99%), Dulbecco's Modified Eagle Medium—high-glucose cell growth medium (DMEM-HG), 1:1 mixture of Dulbecco's Modified Eagle Medium and Ham's F12 cell growth medium (DMEM/F12 1:1), human epidermal growth factor (hEGF; recombinant, expressed in *E. coli*), cholera toxin from *Vibrio cholerae*, bovine insulin (10 mg/mL insulin in 25 mM HEPES, pH 8.2) and hydrocortisone were purchased from Sigma-Aldrich (Sintra, Portugal). Fetal bovine serum (FBS) and horse serum were from Gibco (Thermo Fisher Scientific, Inc., Waltham, MA, USA). Ultrapure water ($18.2 M\Omega \times cm$ at 25 °C) was obtained with an arium[®] pro water purification system (Sartorius, Goettingen, Germany). Animals were anesthetized with isoflurane inhalation (IsoFlo[®], 100% isoflurane) acquired from Abbott (Berkshire, UK). All the other reagents were of analytical grade.

2.2. Pd₂Spm Synthesis and Formulation

The Pd₂Spm complex was synthesized according to published procedures [20] optimized by the authors [21]: 2 mmol of K_2PdCl_4 was dissolved in a minimal amount of water and 1 mmol of spermine aqueous solution was added dropwise under continuous stirring. After 24 h, the resulting orange powder was filtered and washed with acetone, and the yellow-orange needle-shaped crystals were recrystallized from water. The composition and purity of the synthesized compound were fully obtained by elemental analysis and vibrational spectroscopy (FTIR, Raman and inelastic neutron scattering), which were compared with the previously calculated vibrational profiles (by ab initio methods) [21,22]. Yield: 68%. Elemental analysis (Pd₂(C₁₀N₄H₂₆)Cl₄): Found—C: 21.2%; H: 4.7%; N: 9.6%, Cl: 25.9%; Calculated—C: 21.5%; H: 4.6%; N: 9.9%, Cl: 25.6%. A Pd₂Spm 0.28 mg/mL solution for in vivo administration was freshly prepared by dissolving an appropriate quantity of drug in phosphate-buffered saline (PBS) (H₂PO₄ 1.5 mM, Na₂HPO₄ 4.3 mM, KCl 2.7 mM, NaCl 150 mM, pH 7.4) containing 0.5% of DMSO and sterile-filtered. A solution of cisplatin 0.35 mg/mL was prepared in PBS and sterile-filtered.

2.3. Cell Cultures

The human triple-negative breast cancer cell line MDA-MB-231 (ATCC HTB-26) (absence of estrogen and progesterone receptors, HER2 overexpression) and the non-cancerous breast cell line MCF-12A (ATCC CRL-10782) were purchased from ATCC (Manassas, VA, USA). MDA-MB-231 cells were cultured in DMEM-HG cell growth medium supplemented with 10% (*v/v*) FBS. MCF-12A cells were cultured in DMEM/F12 medium supplemented with 20 ng/mL hEGF, 100 ng/mL cholera toxin, 0.01 mg/mL bovine insulin, 500 ng/mL hydrocortisone and 5% (*v/v*) horse serum. Cells were cultured in monolayers in a sterile environment at 37 °C with 5% CO₂ humidified atmosphere. Under these conditions, the population doubling time was 25.5 ± 0.9 h and 20.6 ± 3.1 h for MDA-MB-231 and MCF-12A cells, respectively. The cell cultures were routinely screened for mycoplasma contamination, yielding negative results.

2.4. Cell Proliferation Assay

Cells were seeded in 96-well microplates at the cell density 1.5×10^4 cells/cm² (final volume 200 μ L/well) and left 24 h to attach. Afterwards, the growth medium was replaced with the growth medium containing Pd₂Spm (1–100 μ M) or cisplatin (0.1–100 μ M). Label-free kinetic live monitoring of cell proliferation was performed using LionheartFX automated microscope (BioTek, Winooski, VT, USA) with direct image acquisition of cells in microplates at 0, 24, 48 and 72 h post-addition of the tested compounds. Acquired 4X images were processed using Gen 5 Image Analysis software (BioTek, Winooski, VT, USA) that allows for identification and counting of individual cells per image. The normalized cell growth (%) was calculated using the following formula:

$$C(t) = [(\text{Number of Treated Cells}(t) - \text{Number of Treated Cells}(0)) / (\text{Number of Untreated Cells}(t) - \text{Number of Untreated Cells}(0))] \times 100,$$

where $C(t)$ is the percent of net cell growth over time, Number of Treated Cells(t) is the count of cells treated with drug at each time point, Number of Treated Cells(0) is the count of cells treated with drug at time 0 h, Number of Untreated Cells(t) is the count of untreated (control) cells at each time point, Number of Untreated Cells(0) is the count of untreated (control) cells at time 0 h.

2.5. Cell Migration—Wound Healing Assay

The effect of compounds on cell migration was studied using wound healing assay (or scratch assay). Triple-negative breast cancer MDA-MB-231 cells were seeded in 24-well microplate at the cell density 12.5×10^4 cells/cm² (1 mL final volume) and left 24 h to attach and create a confluent monolayer. The cell monolayer was scratched with 200 μ L pipette tip, producing a vertical straight wound in the middle of the well; growth medium was removed and wells were washed twice with growth medium to remove all detached cells. Growth medium containing Pd₂Spm (12.5–200 μ M) or cisplatin (6.25–200 μ M) was added to the wells, and microplates were imaged using LionheartFX automated microscope at 0, 3, 18, 20, 24 and 48 h. Wound closure was analyzed as a confluence of the initial cell-free area covered by migrating cells at the indicated time points measured with Gen 5 Image Analysis software. Confluence was calculated using the following formula:

$$C(t) = [(\text{Object Sum Area}(t) - \text{Object Sum Area}(0)) / (I(A) - \text{Object Sum Area}(0))] \times 100,$$

where $C(t)$ is the percent wound confluence over time, Object Sum Area(t) is the area covered by cells at each time point, Object Sum Area(0) is the area covered by cells at time 0 h and $I(A)$ is the total area of the 4X image. The area under the curve (AUC) of kinetic time–confluence profiles obtained within 0–18 h for each concentration was calculated (AUC_{0–18h}), plotted against the drug concentration and analyzed with nonlinear regression to obtain the half maximal effective concentration (EC₅₀) for Pd₂Spm and cisplatin.

2.6. Quantitative Analysis of Vascular Endothelial Growth Factor (VEGF) Production

MDA-MB-231 cells were seeded in 96-well microplates at the cell density 1.5×10^4 cells/cm² (final volume 200 μ L/well) and left 24 h to attach. The growth medium was replaced with growth medium containing Pd₂Spm (5–20 μ M) or cisplatin (5–20 μ M), and cells were incubated for 12 h. VEGF concentration in cell culture medium was determined in undiluted samples in duplicate using the Human VEGF Quantikine ELISA Kit (R&D Systems Inc., Minneapolis, MN, USA) according to the manufacturer's protocol. In brief, 200 μ L of conditioned media was added to a 96-well microplate pre-coated with monoclonal antibody for human VEGF and the plate was incubated for 2 h. After washing with wash buffer, enzyme-linked polyclonal antibody specific for human VEGF was added, followed by incubation for 2 h. The plate was washed to remove unbound antibody-enzyme reagent, substrate solution was added and incubated for 30 min and the reaction was terminated by the addition of the stop solution, producing a yellow solution. The optical density at 450 nm with wavelength correction at 540 nm was measured using a Synergy HT microplate reader (BioTek, Winooski, VT, USA). The concentration of VEGF was interpolated from the standard curve (15.6–1000 pg/mL) prepared in parallel.

2.7. Mice

Female CBA nude (N:NIH(S)II-nu/nu) mice (6–7 weeks old, 21 animals in total) with combined immunodeficiency [23] were purchased from i3S Animal Facility (Porto, Portugal). Animals were acclimatized at ICBAS-UP Rodent Animal House Facility (Porto, Portugal) at least one week prior to the experiments, were randomly distributed into groups of three per individually ventilated cage and were housed under controlled specific-

pathogen-free (SPF) environmental conditions (temperature 22.5 ± 1.5 °C; relative humidity $50 \pm 10\%$; 12 h light/dark cycle) with ad libitum access to water and standard pellet food (4RF21, Mucedola, Italy). Environmental enrichment included corncob bedding, paper roll tube and one large sheet of tissue paper for nesting. Animals were monitored daily for health status and welfare.

2.8. Subcutaneous In Vivo Breast Cancer Xenograft Study

Mice were subcutaneously implanted in the left flank with breast cancer MDA-MB-231 cells (25G needle, 5×10^6 cells in 150 μ L of PBS). At day 25 post-implantation, when tumors reached a mean volume of ~ 250 mm³, mice were randomly allocated into three groups (7 animals per group) using computer-generated randomization sequence followed by random group allocation to the treatment with either (A) Pd₂Spm, (B) cisplatin or (C) vehicle. The Pd₂Spm (5 mg/kg/day), cisplatin (2 mg/kg/day) or vehicle (PBS + 0.5% DMSO) were administered via intraperitoneal injection (500 μ L injection volume) during five consecutive days in the A) Pd₂Spm, B) cisplatin and C) vehicle group, respectively. The animals were monitored daily for physical activity, wellbeing and measurements of body weight. Tumor measurements were performed by two independent researchers using a digital caliper in two perpendicular diameters of the implant. Tumor volumes were calculated using the Carlsson formula [24]: tumor volume (mm³) = $0.5 \times$ largest diameter (mm) \times smallest diameter² (mm). Researchers were blinded to treatment allocation while performing outcome measurements. At day 39 post-implantation (end of the study), animals were euthanized with isoflurane followed by cardiac puncture for blood collection. Blood was collected into K3EDTA tubes for hematological and biochemical analyses. Brain, heart, lungs, liver, kidneys, spleen, inguinal lymphatic nodes and tumor were excised, washed in PBS and weighed. Two animals from the vehicle group developed ulcerated tumors during the treatment period (day 28 post-implantation); thus, these animals were euthanized and excluded from the study.

2.9. Histological Analysis and Immunohistochemistry

Animal tissues were fixed in 10% buffered formalin, routinely processed and embedded in paraffin wax. Serial sections with 2 μ m thickness were cut from each paraffin block; one section was stained with hematoxylin–eosin for histological examination, and the others were used for immunohistochemistry. Histological grading of the mammary carcinomas was performed according to the Nottingham histological grading method [25] based on a semi-quantitative assessment of three histological parameters: tubular formation, nuclear pleomorphism and mitotic figures count. The score of these parameters is used to assign the tumor grade: grade I (well-differentiated tumors), grade II (moderately differentiated tumors) or III (poorly differentiated tumors).

For the immunohistochemical study, tissue sections were dewaxed and rehydrated. Slides were submitted to proteolytic digestion by immersion in 10% retrieval solution (Dako) and kept in a water bath at 100 °C for 20 min. After blocking of non-specific staining, slides were incubated with primary antibody for Ki-67 (1:50 dilution, clone MIB-1, Dako) overnight at 4 °C. Slides were then stained with Novolink Polymer Detection Systems (Leica Biosystems Inc., Buffalo Grove, IL, USA) following manufacturer's instructions, counterstained with hematoxylin and permanently mounted. The nuclear Ki-67 staining was analyzed using Fiji's high-throughput automatic quantitation with Andy's Algorithm pipeline, as described elsewhere [26]. The immunoreactivity was evaluated, counting at least 600 nuclei/field from 5 representative fields of the lesion at high magnification, avoiding necrotic areas. The ratio of Ki-67 positive nuclei per all counted nuclei was expressed as a percentage (Ki-67 proliferation index).

2.10. Detection of Apoptosis with Labeling of DNA Strand Breaks (TUNEL Assay)

The paraffin-embedded tumor sections were deparaffinized, rehydrated through a graded series of ethanol and double distilled water and then stained with In Situ Cell Death

Detection Kit (Roche Diagnostics GmbH, Mannheim, Germany) as per manufacturer's instructions. Apoptosis was quantified at single-cell level by counting the number of cells positive for terminal deoxynucleotidyl transferase (TdT) dUTP nick-end labeling (TUNEL-positive cells). Briefly, tumor sections were incubated with 20 µg/mL proteinase K solution (in 10 mM Tris/HCl, pH 7.4–8) for 30 min at 37 °C. Slides were washed and stained with TUNEL reaction mixture (mixture of terminal deoxynucleotidyl transferase with labeled nucleotides) for 60 min at 37 °C in the dark followed by three washes. Slides were mounted with VECTASHIELD Antifade Mounting Medium with DAPI, and coverslips were sealed. At least twenty nonoverlapping high-power microscope fields of each tumor section were captured while avoiding areas with central necrosis. Fluorescence images were acquired using the LionHeart automated microscope at Ex: 520–560 nm and Em: 570–620 nm.

2.11. Biochemical and Hematological Analyses

Red blood cells (RBC), hemoglobin (Hb), hematocrit (Hct), mean corpuscular volume (MCV) and mean corpuscular hemoglobin (MCH) were analyzed in a small aliquot of whole blood using ABX Micros 60 automated analyzer (Horiba ABX SAS, Montpellier, France). The remaining blood was centrifuged at 900× g for 15 min, and plasma was separated into aliquots and frozen at −80 °C for biochemical assays. Plasma parameters were analyzed using commercial kits for aspartate aminotransferase—AST (AST CP, A11A01629), alanine transaminase—ALT (ALT CP, A11A01627), cholesterol (CHOL CP, A11A01634), creatinine (Creatinine 120 CP, A11A01868), glucose (Glucose PAP CP, A11A01668), total protein (Total protein CP, A11A01669), triglycerides (Triglycerides CP, A11A01640) and urea (Urea CP, A11A01641). All parameters were determined with an automated analyzer Pentra 400 (ABX Horiba diagnostics, Montpellier, France).

2.12. In Vivo CAM Assay

The chicken embryo chorioallantoic membrane (CAM) assay was used to study the effect of tested drugs on neovascularization, as described elsewhere [27]. Briefly, fertilized chicken eggs were incubated at 37.5 °C in a humidified atmosphere with agitation. After 3 days of incubation, 2.5 mL of albumen was removed to detach developing CAM from the shell. A window in the eggshell was cut off to expose the embryo, and then, the eggshell was sealed with paraffin. Incubation of fertilized eggs continued until day 9, when the windows were unsealed and four paper disks previously sterilized and pre-treated with hydrocortisone (a cyclooxygenase inhibitor to avoid inflammatory responses) were placed in direct contact with CAM in each egg (3 PBS-soaked disks and 1 VEGF-soaked (10 ng/mL) disk), and windows were re-sealed with paraffin. On day 11, two of the PBS-soaked disks were treated with Pd₂Spm (2 to 8 µM) or cisplatin (2 to 8 µM). The remaining two disks were used as negative/vehicle (treated with PBS) and positive (treated with VEGF) controls. The eggs were further incubated two more days, and at day 13, the disks bound to the CAM were removed, placed in PBS and imaged using a contrast-phase microscope (Motic® AE200 inverted microscope, Spectra Services, VWR International) (with a 4X magnification) coupled to a Moticam 5 digital camera. Images were analyzed using the Angiogenesis Analyzer for Fiji [28].

2.13. Ethical Considerations

Handling and care of animals were conducted according to Portuguese (Decreto-Lei n.º 113/2013) and European legislation (Directive 2010/63/EU) on the protection of animals used for scientific purposes and were in agreement with the recommendations in the Guide for Care and Use of Laboratory Animals of the National Institutes of Health (NIH). The study protocol was approved by the Ethics Committee for Animal Experimentation of the Faculty of Pharmacy of the University of Porto, Porto, Portugal (permit number 25-10-2015) and by the Ethics Committee of the local animal welfare body (ICBAS-UP ORBEA, Porto, Portugal) with permit number 134/2015. The ARRIVE Guidelines were followed for reporting in vivo experiments [29].

2.14. Statistical Data Analysis

Data are expressed as mean \pm standard error of the mean (SEM) or medians with corresponding quartiles. Statistical analysis was performed using two-tailed Student's *t*-test or one-way ANOVA followed by Dunnett's multiple comparisons for analysis of means. Changes over the time were analyzed with two-way ANOVA followed by Tukey's multiple comparisons test. Medians were compared with nonparametric Kruskal–Wallis test followed by Dunn's multiple comparisons test. GraphPad Prism 7 Software (San Diego, CA, USA) was used. A *p*-value < 0.05 was considered statistically significant.

3. Results

3.1. Pd₂Spm Showed Selective Antiproliferative Activity for MDA-MB-231 Breast Cancer Cells

The effects of Pd₂Spm and cisplatin on the proliferation of MDA-MB-231 and MCF-12A cells at 24, 48 and 72 h are shown in Figure 1 as dose–response curves. The full range of antiproliferative activity of Pd₂Spm and cisplatin on net cell growth (0–100%) was achieved with the tested concentrations (1 to 100 μ M). For MCF-12A cells, the highest concentration of Pd₂Spm (100 μ M) did not produce a maximum growth inhibition when compared to the same dosage of cisplatin. A clear separation of dose–response curves obtained for MDA-MB-231 and MCF-12A cells was observed for Pd₂Spm at 24, 48 and 72 h incubation periods. For cisplatin, an overlap between the dose–response curves for MDA-MB-231 and MCF-12A was detected at these time points. Nonlinear regression analysis of dose–response curves was used to compute the half maximal inhibitory concentration (IC₅₀) for Pd₂Spm and cisplatin (Table 1). For Pd₂Spm, the IC₅₀ values obtained in MDA-MB-231 cells were significantly lower than the IC₅₀ values determined in MCF-12A cells, suggesting lower sensitivity of non-cancerous MCF-12A to Pd₂Spm. For cisplatin, on the other hand, the IC₅₀ obtained for MDA-MB-231 and MCF-12A cells did not show significant differences, which is indicative of non-discriminatory antiproliferative effects elicited by cisplatin.

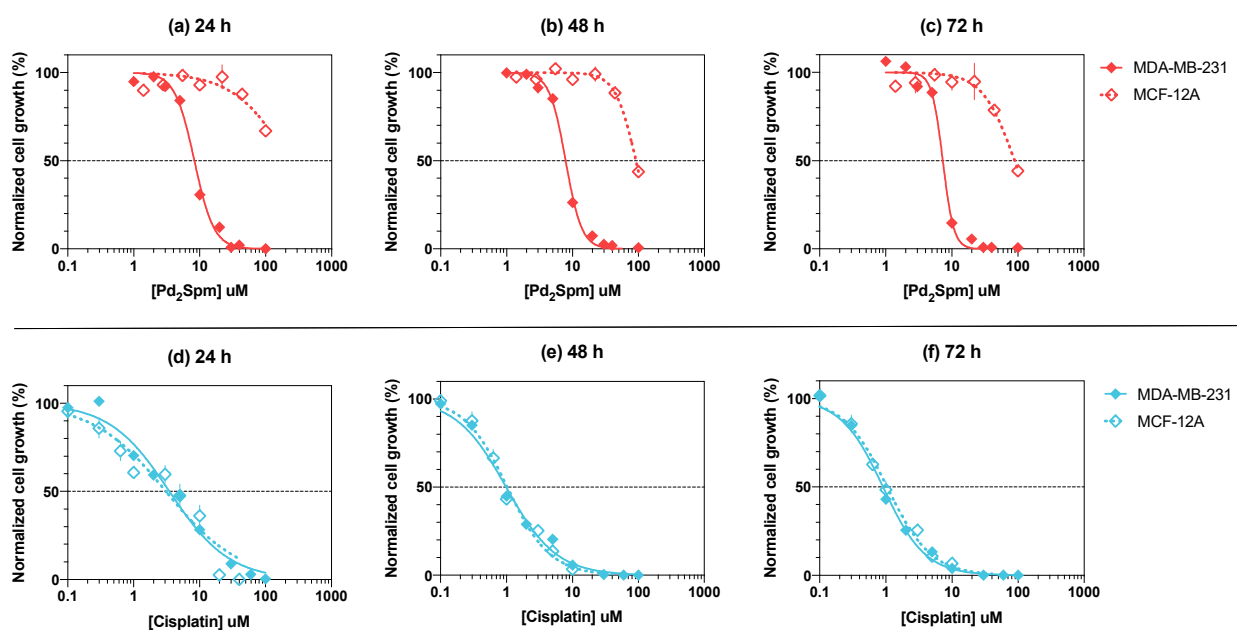


Figure 1. Dose–response curves of Pd₂Spm (red, a–c) and cisplatin (blue, d–f) in breast cancer (MDA-MB-231, solid line) and non-cancer (MCF-12A, dotted line) cells at 24, 48 and 72 h of incubation. Data are expressed as mean \pm SEM, *n* = 4. Data points with no visible error bars have errors smaller than the size of the symbol.

Table 1. The half maximal inhibitory concentration (IC₅₀) of Pd₂Spm and cisplatin in triple-negative human breast cancer (MDA-MB-231) and non-cancer breast (MCF-12A) cells at 24, 48 and 72 h of incubation.

Drug	Time	MDA-MB-231		MCF-12A		<i>p</i> -Value ^a
		IC ₅₀ in μM [95% CI]	logIC ₅₀ ± SEM	IC ₅₀ in μM [95% CI]	logIC ₅₀ ± SEM	
Pd ₂ Spm	24 h	8.3 [7.4–9.3]	−5.081 ± 0.024	228.9 [107.9–1144.12]	−3.640 ± 0.215	0.0006
	48 h	7.9 [7.1–8.8]	−5.105 ± 0.022	91.5 [81.5–104.3]	−4.039 ± 0.023	<0.0001
	72 h	7.3 [6.6–8.0]	−5.137 ± 0.021	89.5 [66.4–159.0]	−4.048 ± 0.068	<0.0001
Cisplatin	24 h	3.5 [2.9–4.1]	−5.459 ± 0.036	3.1 [2.3–4.1]	−5.510 ± 0.062	0.5308
	48 h	1.0 [0.9–1.1]	−6.005 ± 0.027	1.0 [0.9–1.1]	−5.988 ± 0.029	0.6954
	72 h	0.9 [0.8–1.0]	−6.043 ± 0.020	1.0 [0.9–1.2]	−5.981 ± 0.026	0.1176

IC₅₀ values are expressed in μM with corresponding 95% confidence intervals and as mean logIC₅₀ ± SEM, *n* = 4;
^a Student's *t*-test comparison of logIC₅₀ means between the two cell lines at a specified time.

3.2. Pd₂Spm Inhibited In Vitro Migration of MDA-MB-231 Cells

The effects of Pd₂Spm and cisplatin on the migration of MDA-MB-231 cells is depicted in Figure 2. The kinetic profiles (between 0 and 48 h) of migrating cells exposed to different concentrations of either Pd₂Spm (Figure 2a) or cisplatin (Figure 2b) showed similar dose-dependent effects on cancer cell migration, expressed as a percentage of wound confluency. Untreated cells displayed an almost complete wound closure, reaching a maximum ~100% wound confluence between 18 and 24 h after creation of the scratch in the cell monolayer (Figure 2d). Thus, the area under the curve for the wound confluence–time plot between 0 and 18 h (AUC_{0–18h}) was analyzed (Figure 2c) to reliably capture the drugs' effects on cell migration. The half maximal effective concentrations (EC₅₀) of Pd₂Spm and cisplatin are summarized in Table 2, showing no significant difference in the potency of Pd₂Spm versus cisplatin in inhibiting the migration of MDA-MB-231 cells.

Table 2. Migration of MDA-MB-231 cells (logEC₅₀ values of Pd₂Spm and cisplatin).

Drug	logEC ₅₀	<i>p</i> -Value
Pd ₂ Spm	−4.243 ± 0.113 (57.2)	0.631
Cisplatin	−4.329 ± 0.130 (46.9)	

Data are expressed as mean logEC₅₀ ± SEM (EC₅₀ in μM), *n* = 5.

3.3. Pd₂Spm Administration Inhibited the Growth of MDA-MB-231 Xenografts in Female Nude Mice

To confirm the in vitro findings, we further studied the in vivo effects of intraperitoneal Pd₂Spm administration on the growth of MDA-MB-231 cancer cells subcutaneously implanted in female nude mice. The cisplatin-treated mice were used as a reference treatment group. The selection of doses of Pd₂Spm and cisplatin used in vivo took into consideration the doses we used previously for pharmacokinetic and tissue biodistribution studies [15]. The average tumor volumes in mice treated with either Pd₂Spm (5 mg/kg/day) or cisplatin (2 mg/kg/day) for 5 consecutive days were significantly lower compared to vehicle-treated control mice (*p* < 0.05; Figure 3). At the end of the experiment, the tumor growth reduction (versus the vehicle group) was 43.3% and 56.6% for Pd₂Spm- and cisplatin-treated animals, respectively.

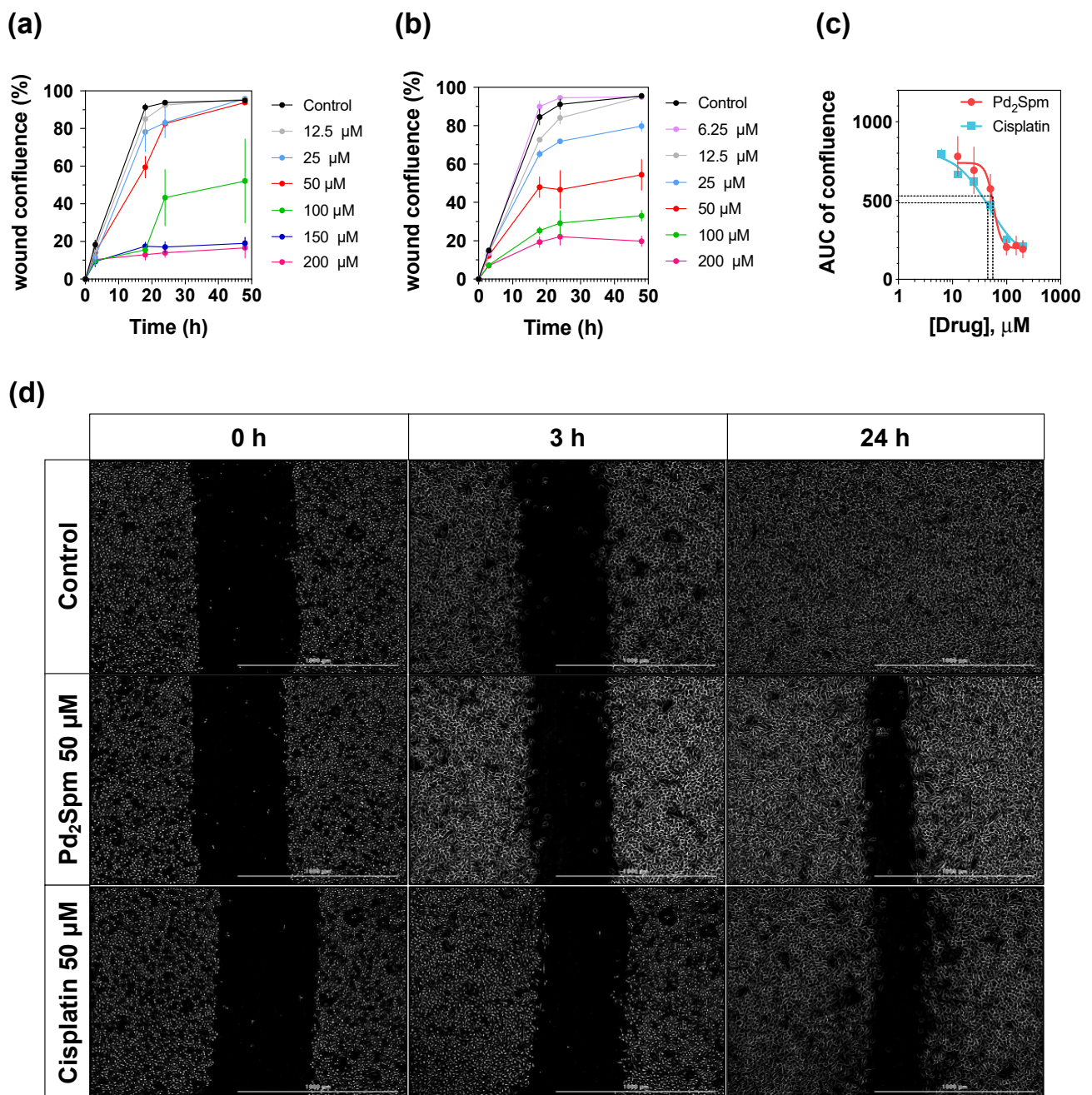


Figure 2. Effects of Pd₂Spm and cisplatin on migration of MDA-MB-231 cells using scratch/wound healing assay. **(a)** Dose-dependent effect of Pd₂Spm on migration of MDA-MB-231 cells expressed as wound confluence for tested Pd₂Spm concentrations. **(b)** Dose-dependent effect of cisplatin on migration of MDA-MB-231 cells expressed as wound confluence for tested cisplatin concentrations. **(c)** Dose-response curve obtained from measuring the area under confluence curve (AUC) between 0 and 18 h of exposure to Pd₂Spm or cisplatin. **(d)** Representative images from 5 independent experiments showing effects of 0 μM (control) and 50 μM of Pd₂Spm or cisplatin on cell migration at 0, 3 and 24 h. Scale bar = 1000 μm. Data are expressed as mean ± SEM, *n* = 5. Data points with no visible error bars have errors smaller than the size of the symbol.

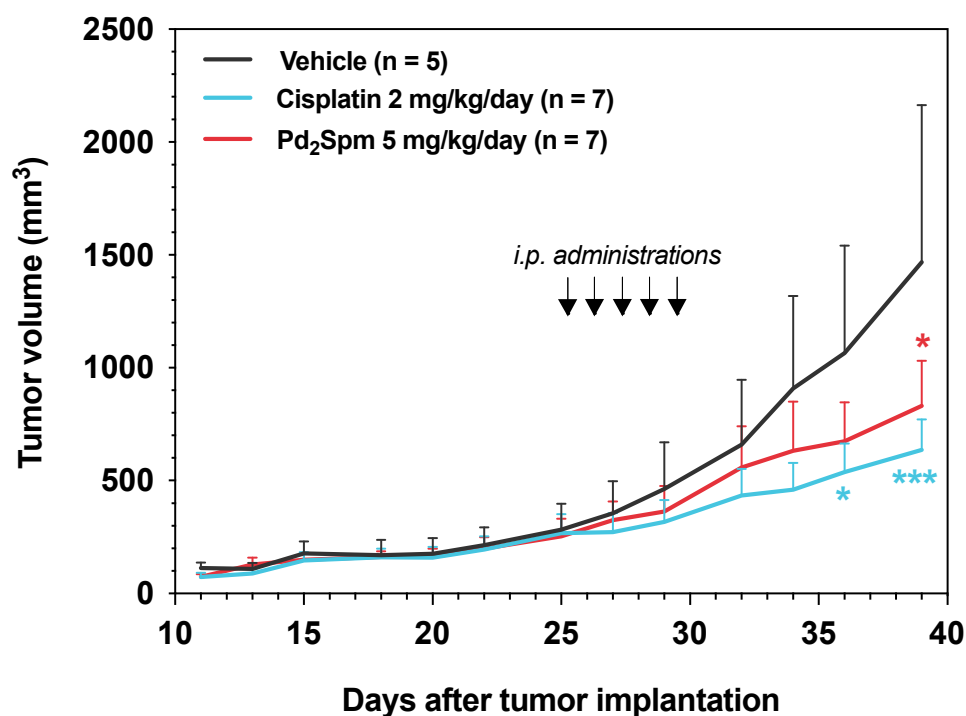


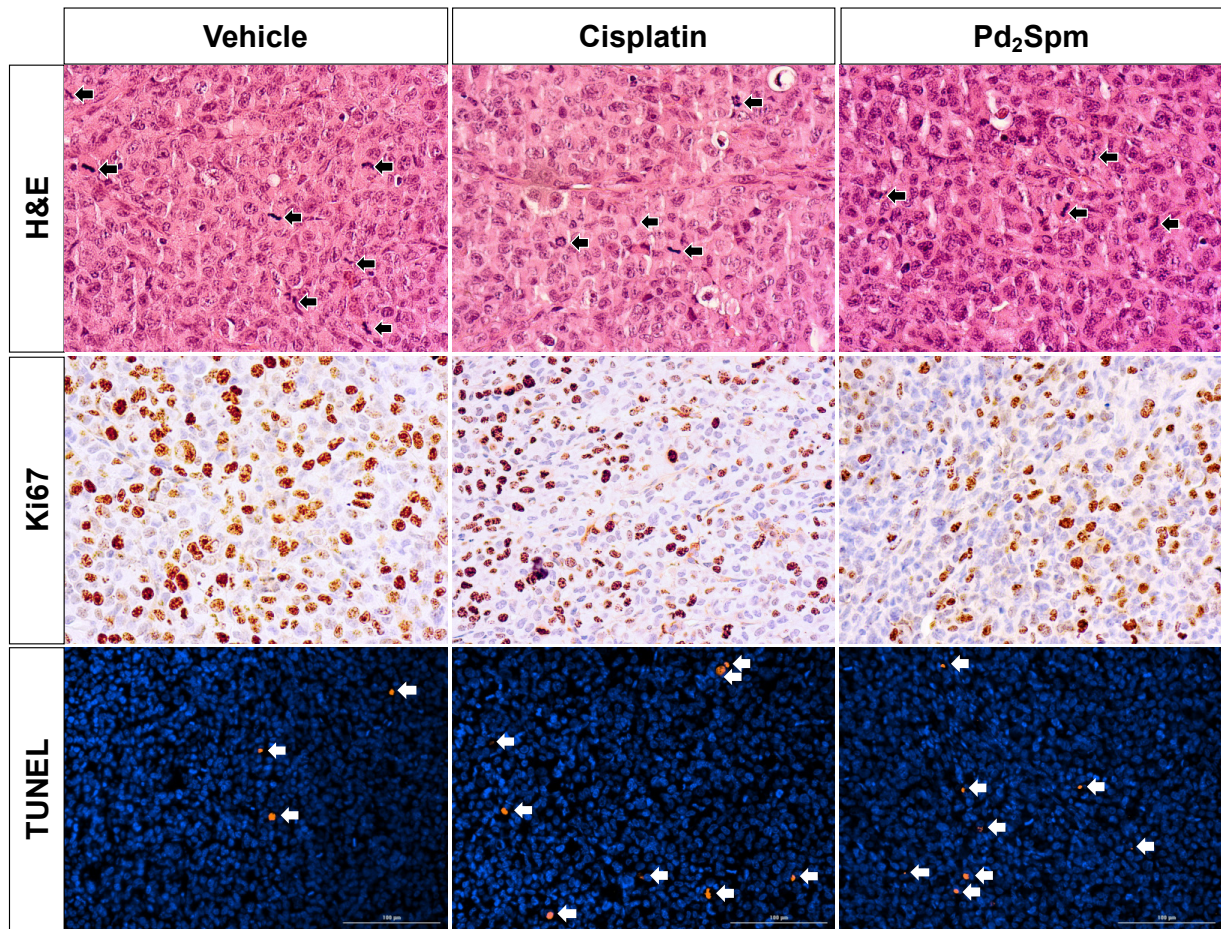
Figure 3. Pd₂Spm suppresses tumor growth of MDA-MB-231 breast cancer xenografts. Graph of the effect of Pd₂Spm treatment (5 mg/kg/day), cisplatin treatment (2 mg/kg/day) or vehicle (PBS + 0.5% DMSO) on MDA-MB-231 tumor volume. Drugs were administered intraperitoneally for 5 consecutive days in CBA nude female mice bearing subcutaneously implanted MDA-MB-231 triple-negative human breast cancer tumors. Data are expressed as mean tumor volume (mm³) ± SEM and analyzed with two-way ANOVA followed by Tukey's multiple comparison test. * $p < 0.05$ Pd₂Spm versus vehicle; *** $p < 0.001$ cisplatin versus vehicle.

3.4. Pd₂Spm Administration Suppressed Cell Proliferation and Induced DNA Damage in Tumors Collected from MDA-MB-231 Breast Tumor-Bearing Mice

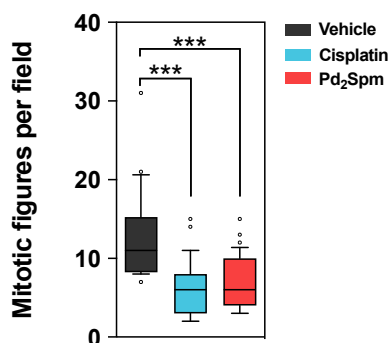
All study animals developed malignant neoplasms characterized by a dense population of polyhedral epithelial cells arranged in a solid pattern. Neoplastic lesions exhibited an infiltrative behavior, infiltrating surrounding muscle and adipose tissue, with large central necrotic areas. Neoplastic cells exhibited marked anisocytosis and anisokaryosis, and multinucleated cells and aberrant nuclear shapes were found (Figure 4a—H&E).

Tumors treated with the vehicle showed highly dense cancer cells with atypical nuclei, evidencing intense mitosis. The mitotic count of vehicle-treated animals was significantly increased compared to cisplatin- and Pd₂Spm-treated groups (Figure 4b). In order to evaluate whether Pd₂Spm-mediated suppression of tumor growth occurred with a decrease in cell proliferation and/or DNA damage induction, the Ki-67 proliferation index (a well-accepted marker of cellular proliferation, [30]) and the TUNEL assay (marker of DNA damage) were used. Immunoreactivity for Ki-67 in tumor sections from the groups of animals under study (Pd₂Spm, cisplatin or vehicle) are shown in Figure 4a. The Ki-67 index of tumors was significantly decreased in animals treated with Pd₂Spm when compared to animals treated with the vehicle. Tumors from cisplatin-treated animals also showed a significant decrease in Ki-67 relative to the vehicle-treated mice (Figure 4c). Analysis of DNA damage showed a significant increase in TUNEL-positive cells in tumors obtained from animals treated with Pd₂Spm and cisplatin when compared to tumors from vehicle-treated animals (Figure 4d).

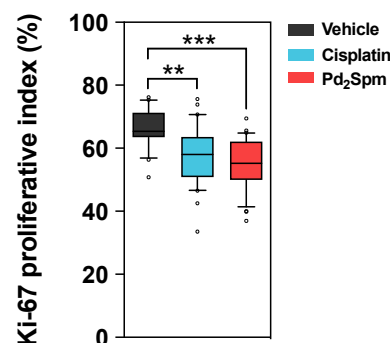
(a)



(b)



(c)



(d)

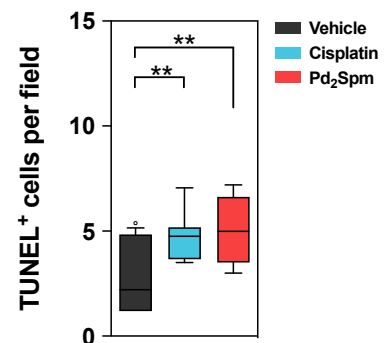


Figure 4. (a) Representative micrographs of MDA-MB-231 breast cancer tumors stained with hematoxylin–eosin (H&E, black arrows show mitotic figures), Ki-67 nuclear staining and TUNEL assay staining (white arrows show TUNEL positive cells). (b) Quantitative analysis of mitotic figures. (c) Quantitative analysis of Ki-67 proliferative index. (d) Quantitative analysis of TUNEL-positive cells. Data are shown as box plots with medians analyzed with Kruskal–Wallis test followed by Dunn’s multiple comparisons test. ** $p < 0.01$, *** $p < 0.001$. Five random fields per tumor with at least 600 cells/field were analyzed. Scale bar = 100 μ m. Pd₂Spm 5 mg/kg/day ($n = 7$), cisplatin 2 mg/kg/day ($n = 7$), vehicle ($n = 5$).

Overall, these results evidenced that Pd₂Spm administration inhibited the growth of MDA-MB-231 xenografts *in vivo* by reducing tumor cell proliferation and inducing DNA damage and cell death. Our data also showed that 5-day treatment of tumor-bearing mice with 5 mg/kg/day of Pd₂Spm or 2 mg/kg/day of cisplatin results in comparable anticancer effects when (i) tumor volume reduction, (ii) tumor proliferative activity decrease (Ki-67 and mitotic count) and (iii) tumor DNA damage increase are compared in Pd₂Spm- versus cisplatin-treated animals. This may be explained in part by the similarity in the pharmacokinetics of Pd₂Spm and cisplatin [15], as well as by the similarity in the amounts of administered metals (1.91 mg/kg/day of palladium administered from 5 mg/kg/day of Pd₂Spm, and 1.3 mg/kg/day of platinum administered from 2 mg/kg/day of cisplatin).

3.5. Impact of Pd₂Spm on the Weight of MDA-MB-231 Breast Tumor-Bearing Mice

As body weight can be considered a marker of general systemic toxicity, we performed a daily monitoring of the mice's weight in all groups. A five-day treatment administration induced notable changes in mice's body weight (Figure 5a): during the initial three days of the treatment, a body weight loss was observed in all study groups, and this trend continued in cisplatin-treated animals also after the administration period. A progressive recovery of the body weight was observed in all groups, and at the end of the experiment, the body weight of all animals was higher compared to the starting value. The cisplatin group demonstrated a slower body weight recovery compared to Pd₂Spm- and vehicle-treated groups. There was no significant difference in body weight between groups at the end of the procedure.

In addition to body weight decrease, cisplatin-treated animals showed signs of general toxicity, such as decreased movement/activity, transient dehydration and diarrhea. In turn, no such adverse effects were observed in animals treated with either Pd₂Spm or the vehicle.

The treatment of animals with Pd₂Spm, cisplatin or vehicle did not impact the relative weight of the liver, heart, lungs, spleen or brain, with no significant differences being detected among the studied groups (Table 3). On the other hand, the relative weight of the kidneys in cisplatin-treated animals was lower compared to animals treated with the vehicle or Pd₂Spm. Histopathological evaluation showed a decreased perirenal adipose tissue in cisplatin-treated compared to vehicle-treated animals, which may further support a reduction in the relative weight of the kidneys in cisplatin-treated animals (Figure 5b). No other histopathological changes were observed during histological analysis of the kidneys (data not shown). Regarding the liver, histopathological analysis allowed us to conclude that cisplatin-treated animals exhibited a swollen, pale and finely vacuolated cytoplasm due to intracellular accumulation of glycogen (Figure 5b), as confirmed by periodic acid–Schiff (PAS). This glycogen accumulation was not observed in the livers of vehicle- and Pd₂Spm-treated animals.

Table 3. Relative organ weight after treatment with either Pd₂Spm, cisplatin or vehicle.

Organ	Relative Organ Weight (%) ^a		
	Vehicle (n = 5)	Cisplatin 2 mg/kg/day (n = 7)	Pd ₂ Spm 5 mg/kg/day (n = 7)
Liver	6.08 ± 0.55	6.50 ± 0.34	6.14 ± 0.29
Heart	0.53 ± 0.06	0.53 ± 0.06	0.53 ± 0.06
Lungs	0.73 ± 0.11	0.77 ± 0.08	0.77 ± 0.08
Spleen	0.31 ± 0.10	0.33 ± 0.08	0.32 ± 0.11
Brain	1.85 ± 0.10	1.79 ± 0.14	1.79 ± 0.16
Kidneys	1.46 ± 0.05	1.29 ± 0.10 *	1.43 ± 0.10

^a The relative organ weight (mean % ± SEM) was calculated as organ weight (g)/body weight (g) × 100%. Data analyzed with one-way ANOVA followed by Dunnett's multiple comparisons *t*-test. * *p* < 0.05 cisplatin versus vehicle.

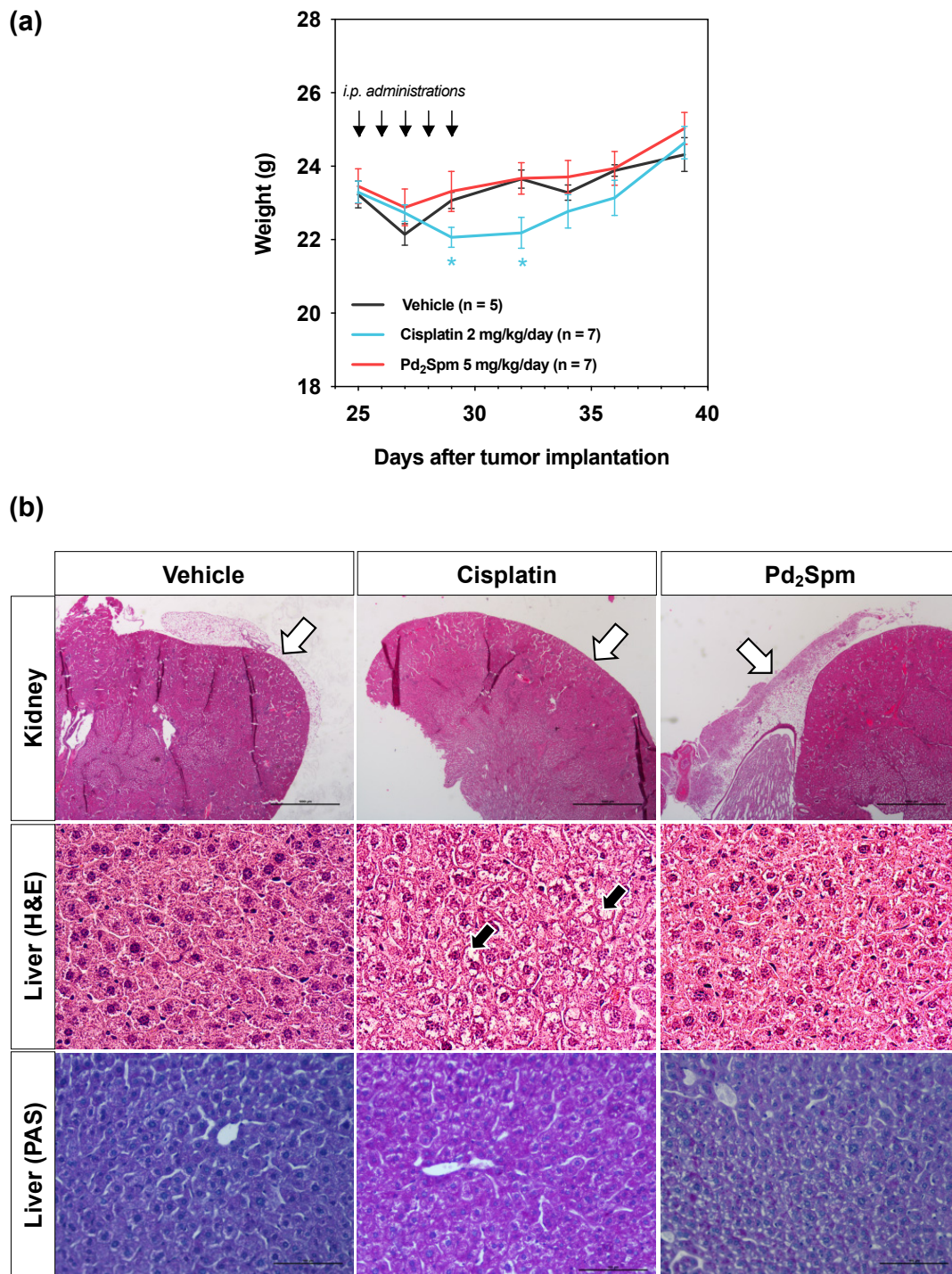


Figure 5. Impact of Pd₂Spm, cisplatin or vehicle treatment on the body weight of MDA-MB-231 breast tumor-bearing mice. (a) Body weight changes of tumor-bearing mice treated intraperitoneally with either Pd₂Spm (5 mg/kg/day), cisplatin (2 mg/kg/day) or vehicle (PBS + 0.5% DMSO) for 5 consecutive days. Data are expressed as mean weight (g) ± SEM. Two-way ANOVA followed by Tukey's multiple comparisons test was used to analyze weight change in groups over the time, * $p < 0.05$ cisplatin versus vehicle. (b) Representative microphotographs of kidney and liver from animals treated with Pd₂Spm, cisplatin or vehicle, showing absence of perirenal adipose tissues (white arrows) in cisplatin-treated animals. Hepatocytes of cisplatin-treated animals showing marked cytoplasmic vacuolization and hepatocellular glycogen deposits (black arrows). Scale bar (kidney) = 1000 μ m. Scale bar (liver) = 100 μ m.

3.6. Impact of Pd₂Spm on the Hematologic and Biochemical Parameters of MDA-MB-231 Breast Tumor-Bearing Mice

Hematologic analysis (RBC, Hb, Htc, MCV, MCH) of animals treated with Pd₂Spm revealed no significant deviations from the animals treated with the vehicle (Figure 6a). Cisplatin-treated animals, in turn, showed a decrease in red blood cells, hemoglobin and hematocrit, accompanied by an increase in the mean corpuscular volume, as compared to vehicle-treated animals. Plasma biochemical analysis (urea, creatinine, glucose, AST, ALT, total proteins, triglycerides and total cholesterol) in Pd₂Spm-treated animals did not reveal changes relative to vehicle-treated animals (Figure 6b). For cisplatin treatment, a decrease in total proteins and an increase in triglycerides were observed as compared to the vehicle-treated group.

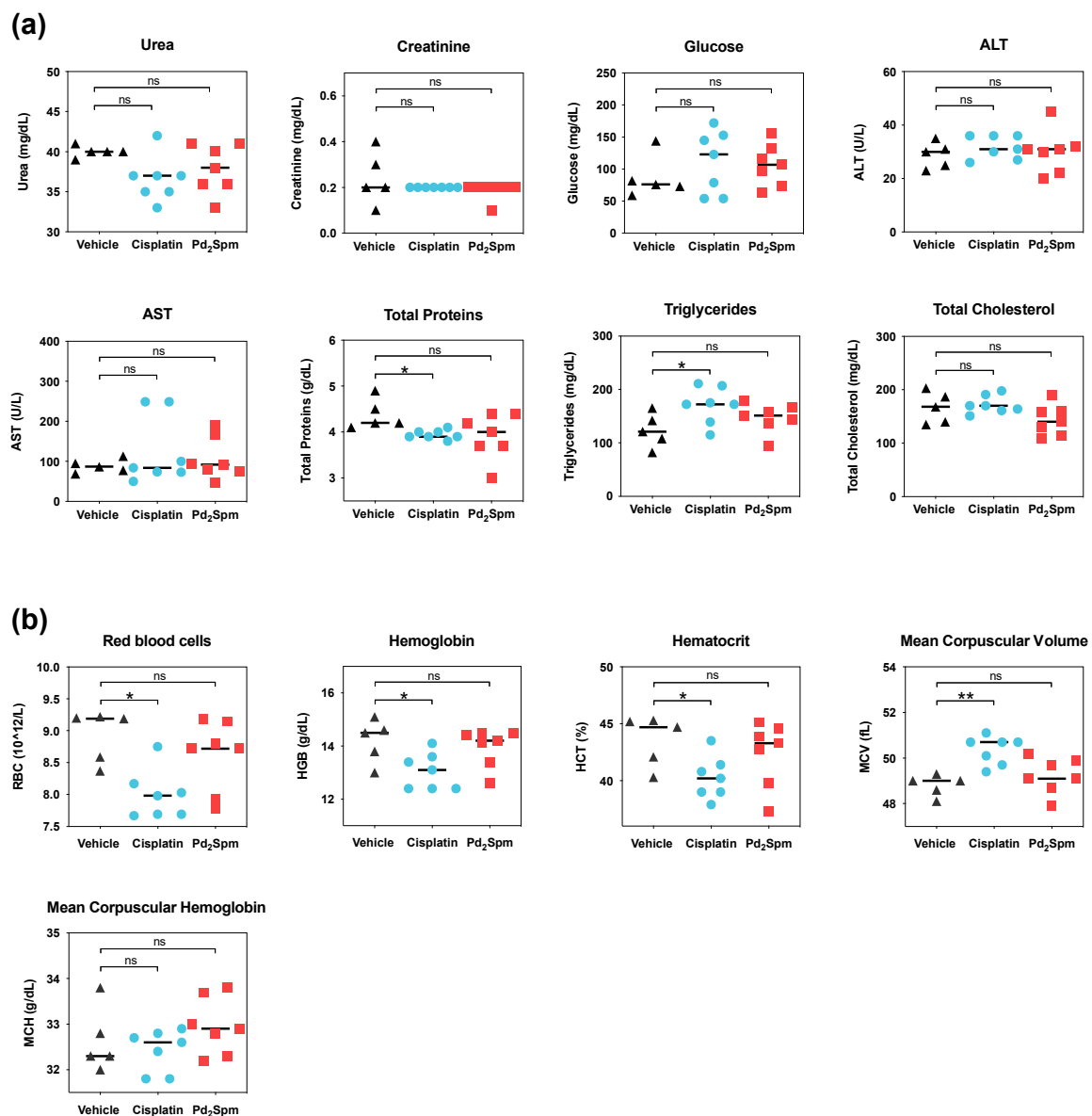


Figure 6. (a) Hematologic analysis and (b) Biochemical analysis of CBA nude female mice bearing subcutaneously implanted MDA-MB-231 triple-negative human breast cancer tumors treated with either Pd₂Spm (5 mg/kg/day), cisplatin (2 mg/kg/day) or vehicle (PBS + 0.5% DMSO). Data are shown as individual values with medians, analyzed with Kruskal–Wallis test followed by Dunn’s multiple comparisons test. * $p < 0.05$, ** $p < 0.01$, ns = not significant. Pd₂Spm ($n = 7$), cisplatin ($n = 5$), vehicle ($n = 5$).

3.7. Pd₂Spm Suppressed Neovascularization in Chorioallantoic Membrane and Reduced VEGF Production in MDA-MB-231 Cells

As angiogenesis plays an important role in the carcinogenesis of TNBC [31], the antiangiogenic potential of Pd₂Spm was investigated and compared to cisplatin. We determined the effect of Pd₂Spm treatment on the neovascularization steps using the CAM assay. Increasing concentrations of Pd₂Spm (2 to 8 μM) and of cisplatin (2 to 8 μM) were able to decrease, in a dose-dependent manner, the number of nodes, junctions and segments, which are parameters associated with the early steps of angiogenesis (Figure 7a). Similarly, Pd₂Spm and cisplatin, in the concentrations tested, reduced, in a dose-dependent manner, the total length, total branching length and total segment length, which are linked to the expansion of newly formed vessels in later steps of angiogenesis (Figure 7b). Thus, these data indicate that both Pd₂Spm and cisplatin have the ability to inhibit angiogenesis, in both the initial and later steps, with a similar potency ($p > 0.05$).

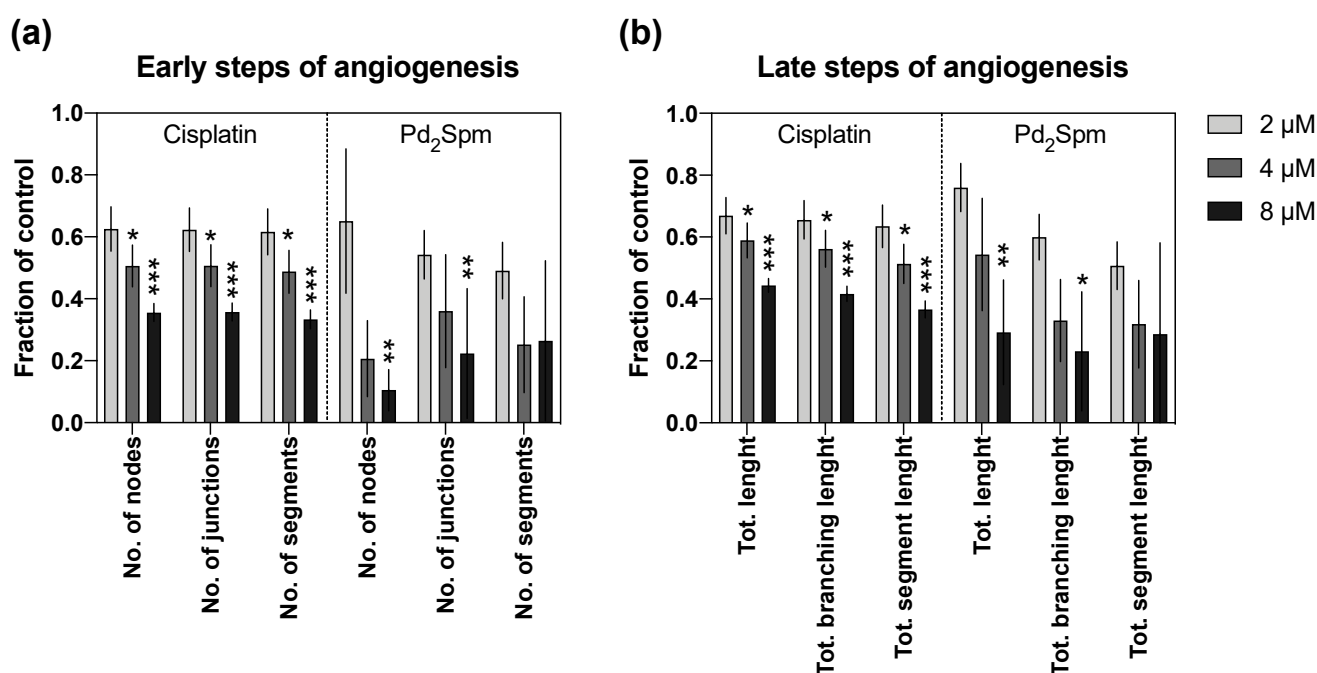


Figure 7. Quantitative results of CAM angiogenesis in the presence of increasing concentrations (2–8 μM) of either cisplatin or Pd₂Spm. (a) Parameters of early steps of angiogenesis: number of nodes, junctions and segments. (b) Parameters of later steps of angiogenesis: total length, branching length and segment length of vessels. The results are expressed as means of the fraction of the control ± SEM from 2 independent experiments ($n = 2, 8$ replicates). Significant differences from the vehicle control: * $p < 0.05$, ** $p < 0.01$, *** $p < 0.001$ (one-way ANOVA followed by Dunnett's multiple comparison test).

Since VEGF plays a crucial role in angiogenesis, we have explored the hypothesis that Pd₂Spm may impact the secretion of VEGF by MDA-MB-231 cells. As shown in Figure 8, both Pd₂Spm (5–20 μM) and cisplatin (5–20 μM) inhibited VEGF secretion in cell culture medium in a dose-dependent manner. Compared to cisplatin, Pd₂Spm incubation resulted in a similar decrease in VEGF secretion by MDA-MB-231.

Together these results indicated that Pd₂Spm may possess anti-angiogenic potential to be further explored and that this effect can be ascribed, at least in part, to its ability to reduce the secretion of VEGF.

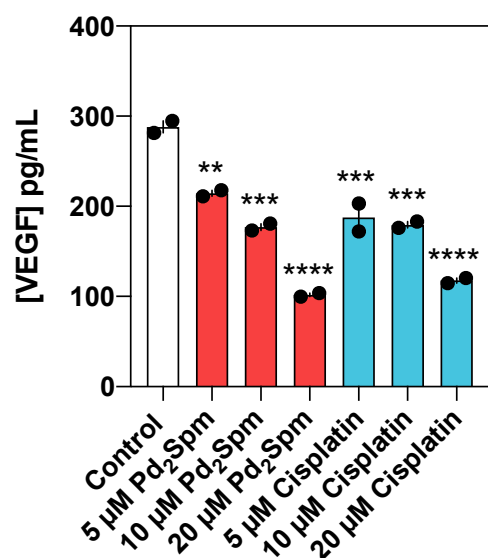


Figure 8. Quantitative results of VEGF secretion by MDA-MB-231 incubated for 12 h with Pd₂Spm (red) or cisplatin (blue). Data are shown as means ± SEM ($n = 2$) and analyzed with one-way ANOVA followed by Dunnett's multiple comparison test. Significant differences from the control: ** $p < 0.01$, *** $p < 0.001$, **** $p < 0.0001$.

4. Discussion

The *in vivo* anticancer effects of Pd₂Spm treatment in mice were studied for the first time, unraveling the promising potential of this dinuclear Pd(II)-polyamine complex regarding its selectivity, efficacy and tolerability as compared to the clinically used Pt(II) drug cisplatin.

The treatment of mice bearing TNBC tumors with 5 mg/kg/day of Pd₂Spm for five days (cumulative dose of 25 mg/kg) induced significant effects: (i) decrease in tumor volume to a similar extent to that observed in animals treated with 2 mg/kg/day of cisplatin (cumulative dose of 10 mg/kg); (ii) reduction in the number of mitoses in the tumor; (iii) decrease in the proliferative index measured with immunohistochemical marker Ki67; and (iv) increase in TUNEL-positive cells (in the tumor), which are indicative of increased DNA damage. The anti-proliferative and selective effects of Pd₂Spm towards TNBC cells was evidenced by the significantly higher IC₅₀ values obtained for non-cancerous MCF-12A cells (89.5–228.9 μM) as compared to MDA-MB-231 cancer cells (7.3–8.3 μM). This ca. 10-fold higher selectivity of Pd₂Spm contrasts with the unselective activity of cisplatin, since this conventional Pt drug shows an equivalent potency towards both MDA-MB-231 and MCF-12A cells. Cisplatin's non-selective antiproliferative activity presently observed corroborates previous reports [32] and may indicate that cisplatin's non-discriminatory effects are responsible for the appearance of off-target toxicity and adverse effects during chemotherapy. For Pd₂Spm, the established selectivity further confirms previous studies performed in human fibroblasts [9] and is a particularly promising result that may lead to a considerable reduction in adverse events during chemotherapy. Additionally, Pd₂Spm consistently shows IC₅₀ values within a low micromolar range in MDA-MB-231 [9,11] and MDA-MB-468 TNBC cells [33], which is a requirement for the successful course towards pre-clinical development and further translation into the clinics. Altogether, these *in vitro* studies sustain the evidence that TNBC is expected to present greater susceptibility to Pd₂Spm than non-TNBC phenotypes, though the molecular mechanisms for these differential effects are yet to be unraveled.

The selectivity and higher tolerability of Pd₂Spm treatment relative to cisplatin was also established from the analysis of the animal welfare, body weight, relative organ weight, histopathological features, hematology and serum biochemistry parameters. Animals treated with Pd₂Spm did not show changes in body weight, gastrointestinal reactivity

(diarrhea) or dehydration, as opposed to animals treated with cisplatin. Moreover, Pd₂Spm administration did not result in significant variations regarding hematological and biochemical parameters when compared to cisplatin-treated animals which evidenced signs of macrocytic anemia (decrease in red blood cells, hemoglobin and hematocrit together with an increase in mean corpuscular volume). The cisplatin-induced changes in body weight, diarrhea and hematotoxicity were previously described [34,35] and are generally considered as surrogates for the drug's systemic toxicity. Furthermore, these results support the reduced off-target effects and low toxicity elicited by Pd₂Spm treatment compared to cisplatin. Interestingly, besides a decrease in the total serum proteins and an increase in serum triacylglycerides, no other parameters related to renal or hepatic functions were altered in cisplatin-treated animals. In contrast, Pd₂Spm treatment did not trigger any of these changes.

Since angiogenesis and cell migration are significant contributors to TNBC pathogenesis, particularly regarding its metastatic potential and aggressive biology, the development of agents able to suppress cancer cell proliferation, migration and angiogenesis are highly desired. In this study, Pd₂Spm-mediated effects against cancer cell invasion yielded promising results since Pd₂Spm: (i) inhibited the migration of MDA-MB-231 cells; (ii) inhibited angiogenesis in CAM; and (iii) suppressed VEGF secretion by MDA-MB-231 cells with similar potency to cisplatin. These results are in line with previous reports that revealed that cisplatin's anti-migratory and antiangiogenic effects, although the underlying mechanism(s) are still largely unknown [36,37]. Regarding the effects of Pd(II) compounds, there is limited information in the literature describing their ability to suppress angiogenesis and cell migration. So far, studies with the mononuclear palladium (II) saccharinate complex of terpyridine [PdCl(terpy)](sac)·2H₂O have shown inhibition of the migration of endothelial cells (HUVEC) in the range of 12.5–50 µM and have also shown inhibition of angiogenesis in CAM assay at a concentration of 5 mg/mL [38]. In the current study, Pd₂Spm significantly inhibited angiogenesis at an 8 µM concentration (corresponding to 4.46 µg/mL of Pd₂Spm), impacting both early and late steps of angiogenesis and further supporting the previous reports [11]. Nevertheless, the mechanism behind this activity is still unexplored and requires further study.

The *in vivo* anticancer activity of Pd(II)-based compounds against TNBC is still largely unexplored, and to date, there are only a few *in vivo* studies in rodents regarding Ehrlich ascites carcinoma (EAC), which is an undifferentiated murine mammary adenocarcinoma sensitive to chemotherapy and not classified as TNBC [39,40]. The Pd complex of terpyridine with saccharinate, also known as [Pd(sac)(terpy)](sac)·4H₂O, administered intraperitoneally at a dose of 2 mg/kg (two injections per week for 2 weeks, up to a cumulative dose of 8 mg/kg) was found to reduce tumor volume by 67.5%, but one mouse died during treatment (1 of 10), indicating the toxicity and poor tolerability of this compound [39]. Another study focused on the similar derivative [PdCl(terpy)](sac)·2H₂O found that at a dose of 3 mg/kg (two injections per week for 2 weeks, up to a cumulative dose of 12 mg/kg), it reduced tumor volume by 69.8%, and one mouse died during treatment (1 of 9) [40]. Additionally, mice treated with 4 mg/kg of cisplatin (two injections per week for 2 weeks up to a cumulative dose of 16 mg/kg) showed 36.4% tumor volume reduction in a first study with two associated deaths [39] and a 46.7% tumor volume reduction in a second study with no associated deaths [40]. When compared to the present results, it is clear that Pd₂Spm shows a good ability to effectively reduce the growth of TNBC tumors by 43.3% at a cumulative dose of 25 mg/kg (5 mg/kg/day of Pd₂Spm for 5 consecutive days) with no associated deaths, while cisplatin reduced the tumor growth by 56.6% at a cumulative dose of 10 mg/kg (2 mg/kg/day of cisplatin for 5 consecutive days). The selection of the 5 mg/kg/day dose of Pd₂Spm accounted for Pd₂Spm's pharmacokinetics and differential accumulation of palladium in cancer cells that were explored in previous studies [15]. Moreover, the dose selection also reflected the different molar ratios of palladium and platinum atoms in Pd₂Spm and cisplatin molecules, respectively (i.e., 5 mg/kg/day of Pd₂Spm corresponded to 1.91 mg/kg/day of the administered dose of palladium, and 2 mg/kg of

cisplatin corresponded to 1.3 mg/kg/day of the administered dose of platinum) [15]. Finally, given the fact that the dose of Pd₂Spm used in this study yielded a promising efficacy and good tolerability, future studies may be focused on a further increase in therapeutic outcomes using different treatment schedules and/or higher Pd₂Spm concentrations.

5. Conclusions

This study constitutes the first proof-of-concept regarding the in vivo activity of Pd₂Spm as a potential candidate chemotherapeutic for TNBC treatment. The in vivo administration of Pd₂Spm in TNBC tumor-bearing mice resulted in tumor growth inhibition to a similar extent to that in animals treated with cisplatin. Furthermore, the systemic toxicity (hematotoxicity, weight loss, diarrhea and biochemical alterations) observed in cisplatin-treated animals was not verified in Pd₂Spm-treated mice. Here we have provided encouraging evidence of the selective activity of Pd₂Spm towards TNBC with minimal effects to non-cancerous breast cells, both in vitro and in vivo. Therefore, Pd₂Spm may become a promising potential Pd(II) drug candidate for the treatment of TNBC.

Author Contributions: Conceptualization, M.V., S.G.-M., M.P.M.M., H.M.-F., I.M.P.L.V.O.F. and C.D.; methodology (synthesis and characterization of Pd₂Spm), A.L.M.B.d.C.; methodology (in vitro and in vivo), M.V., S.G.-M. and C.D.; validation, M.V. and S.G.-M.; formal analysis, M.V.; investigation, M.V., S.G.-M., P.Š., K.V., L.B., F.M. and P.D.-P.; data curation, M.V.; writing—original draft preparation, M.V., M.P.M.M., P.D.-P. and C.D.; writing—review and editing, all authors; visualization, M.V.; supervision, M.P.M.M., H.M.-F., I.M.P.L.V.O.F. and C.D.; project administration, M.P.M.M., I.M.P.L.V.O.F. and C.D.; funding acquisition, M.P.M.M., I.M.P.L.V.O.F. and C.D. All authors have read and agreed to the published version of the manuscript.

Funding: The Portuguese Foundation for Science and Technology (FCT) is acknowledged for UIDB/QUI/50006/2020, UIDB/00070/2020 and PTDC/QEQ-MED/1890/2014 (within Project 3599—to promote scientific production and technological development as well as the formation of thematic networks (3599-PPCDT)—jointly financed by the European Community Fund and FEDER).

Institutional Review Board Statement: The study was approved by the Institutional Ethics Committee of Faculty of Pharmacy of the University of Porto (permit number 25-10-2015) and by the Ethics Committee of the local animal welfare body (ICBAS-UP ORBEA, Porto, Portugal) with permit number 134/2015.

Informed Consent Statement: Not applicable.

Data Availability Statement: The data presented in this study are available on request from the corresponding author (M.V.).

Acknowledgments: Martin Vojtek thanks the Portuguese Foundation for Science and Technology (FCT) and the PhD Program in Medicines and Pharmaceutical Innovation (i3DU) for PhD Grant PD/BD/135460/2017, funded by the European Social Fund of the European Union and national funds FCT/MCTES. The authors thank Sara Capas-Peneda for procedural support and valuable recommendations during the in vivo experiments. We also thank Bárbara Duarte, Rita Ribeiro-Oliveira, Anabela Costa, Maria do Céu Pereira, Mónica Caldas and Sara Cravo for their technical assistance.

Conflicts of Interest: The authors declare no conflict of interest. The funders had no role in the design of the study; in the collection, analyses or interpretation of data; in the writing of the manuscript; or in the decision to publish the results.

References

1. Sung, H.; Ferlay, J.; Siegel, R.L.; Laversanne, M.; Soerjomataram, I.; Jemal, A.; Bray, F. Global Cancer Statistics 2020: GLOBOCAN Estimates of Incidence and Mortality Worldwide for 36 Cancers in 185 Countries. *CA Cancer J. Clin.* **2021**, *71*, 209–249. [[CrossRef](#)]
2. Wu, Q.; Siddharth, S.; Sharma, D. Triple Negative Breast Cancer: A Mountain Yet to Be Scaled Despite the Triumphs. *Cancers* **2021**, *13*, 3697. [[CrossRef](#)]
3. Bianchini, G.; De Angelis, C.; Licata, L.; Gianni, L. Treatment Landscape of Triple-Negative Breast Cancer—Expanded Options, Evolving Needs. *Nat. Rev. Clin. Oncol.* **2021**, *274*. [[CrossRef](#)]
4. Manjunath, M.; Choudhary, B. Triple-negative Breast Cancer: A Run-through of Features, Classification and Current Therapies (Review). *Oncol. Lett.* **2021**, *22*, 512. [[CrossRef](#)]

5. Yang, R.; Shi, Y.-Y.; Han, X.-H.; Liu, S. The Impact of Platinum-Containing Chemotherapies in Advanced Triple-Negative Breast Cancer: Meta-Analytical Approach to Evaluating Its Efficacy and Safety. *Oncol. Res. Treat.* **2021**, *44*, 333–343. [[CrossRef](#)]
6. Crona, D.J.; Faso, A.; Nishijima, T.F.; McGraw, K.A.; Galsky, M.D.; Milowsky, M.I. A Systematic Review of Strategies to Prevent Cisplatin-Induced Nephrotoxicity. *Oncologist* **2017**, *22*, 609. [[CrossRef](#)]
7. Vojtek, M.; Marques, M.P.M.; Ferreira, I.M.P.L.V.O.; Mota-Filipe, H.; Diniz, C. Anticancer Activity of Palladium-Based Complexes against Triple-Negative Breast Cancer. *Drug Discov. Today* **2019**, *24*, 1044–1058. [[CrossRef](#)] [[PubMed](#)]
8. Martins, A.S.; Batista de Carvalho, A.L.M.; Lamego, I.; Marques, M.P.M.; Gil, A.M. Cytotoxicity of Platinum and Palladium Chelates against Osteosarcoma. *ChemistrySelect* **2020**, *5*, 5993–6000. [[CrossRef](#)]
9. Fiuza, S.M.; Holy, J.; Batista de Carvalho, L.A.E.; Marques, M.P.M. Biologic Activity of a Dinuclear Pd(II)-Spermine Complex Toward Human Breast Cancer. *Chem. Biol. Drug Des.* **2011**, *77*, 477–488. [[CrossRef](#)]
10. Tummala, R.; Diegelman, P.; Fiuza, S.M.; Batista de Carvalho, L.A.E.; Marques, M.P.M.; Kramer, D.L.; Clark, K.; Vujcic, S.; Porter, C.W.; Pendyala, L. Characterization of Pt-, Pd-Spermine Complexes for Their Effect on Polyamine Pathway and Cisplatin Resistance in A2780 Ovarian Carcinoma Cells. *Oncol. Rep.* **2010**, *24*, 15–24. [[CrossRef](#)] [[PubMed](#)]
11. Batista de Carvalho, A.L.M.; Medeiros, P.S.C.; Costa, F.M.; Ribeiro, V.P.; Sousa, J.B.; Diniz, C.; Marques, M.P.M. Anti-Invasive and Anti-Proliferative Synergism between Docetaxel and a Polynuclear Pd-Spermine Agent. *PLoS ONE* **2016**, *11*, e0167218. [[CrossRef](#)]
12. Farrell, N.P. Multi-Platinum Anti-Cancer Agents. Substitution-Inert Compounds for Tumor Selectivity and New Targets. *Chem. Soc. Rev.* **2015**, *44*, 8773–8785. [[CrossRef](#)]
13. Allardyce, C.S.; Dyson, P.J. Metal-Based Drugs That Break the Rules. *Dalt. Trans.* **2016**, *45*, 3201–3209. [[CrossRef](#)] [[PubMed](#)]
14. Marques, M.P.M. Platinum and Palladium Polyamine Complexes as Anticancer Agents: The Structural Factor. *ISRN Spectrosc.* **2013**, *2013*, 1–29. [[CrossRef](#)]
15. Vojtek, M.; Gonçalves-Monteiro, S.; Pinto, E.; Kalivodová, S.; Almeida, A.; Marques, M.P.M.; de Carvalho, A.L.M.B.; Martins, C.B.; Mota-Filipe, H.; Ferreira, I.M.P.L.V.O.; et al. Preclinical Pharmacokinetics and Biodistribution of Anticancer Dinuclear Palladium(II)-Spermine Complex (Pd2Spm) in Mice. *Pharmaceuticals* **2021**, *14*, 173. [[CrossRef](#)] [[PubMed](#)]
16. Marques, M.P.M.; Batista De Carvalho, A.L.M.; Sakai, V.G.; Hatter, L.; Batista De Carvalho, L.A.E. Intracellular Water-an Overlooked Drug Target? Cisplatin Impact in Cancer Cells Probed by Neutrons. *Phys. Chem. Chem. Phys.* **2017**, *19*, 2702–2713. [[CrossRef](#)] [[PubMed](#)]
17. Marques, M.P.M.; Batista de Carvalho, A.L.M.; Mamede, A.P.; Dopplapudi, A.; Rudić, S.; Tyagi, M.; Garcia Sakai, V.; Batista de Carvalho, L.A.E. A New Look into the Mode of Action of Metal-Based Anticancer Drugs. *Molecules* **2020**, *25*, 246. [[CrossRef](#)]
18. Marques, M.P.M.; Batista de Carvalho, A.L.M.; Mamede, A.P.; Rudić, S.; Dopplapudi, A.; Garcia Sakai, V.; Batista de Carvalho, L.A.E. Intracellular Water as a Mediator of Anticancer Drug Action. *Int. Rev. Phys. Chem.* **2020**, *39*, 67–81. [[CrossRef](#)]
19. Carneiro, T.J.; Araújo, R.; Vojtek, M.; Gonçalves-Monteiro, S.; Diniz, C.; de Carvalho, A.L.M.B.; Marques, M.P.M.; Gil, A.M. Novel Insights into Mice Multi-Organ Metabolism upon Exposure to a Potential Anticancer Pd(II)-Agent. *Metabolites* **2021**, *11*, 114. [[CrossRef](#)] [[PubMed](#)]
20. Codina, G.; Caubet, A.; López, C.; Moreno, V.; Molins, E. Palladium(II) and Platinum(II) Polyamine Complexes: X-Ray Crystal Structures of (SP-4-2)-Chloro[N-[(3-Amino-KN) Propyl]Propane-1,3-Diamine- KN,KN'}palladium(1+) Tetrachloropalladate (2-) (2:1) and (R,S)- Tetrachloro[μ-(Spermine)]Dipalladium(II) (=μ-{N,N'}. *Helv. Chim. Acta* **1999**, *82*, 1025–1037. [[CrossRef](#)]
21. Fiuza, S.M.; Amado, A.M.; Parker, S.F.; Marques, M.P.M.; Batista De Carvalho, L.A.E. Conformational Insights and Vibrational Study of a Promising Anticancer Agent: The Role of the Ligand in Pd(II)-Amine Complexes. *New J. Chem.* **2015**, *39*, 6274–6283. [[CrossRef](#)]
22. Batista de Carvalho, L.A.E.; Marques, M.P.M.; Martin, C.; Parker, S.F.; Tomkinson, J. Inelastic Neutron Scattering Study of Pt^{II} Complexes Displaying Anticancer Properties. *ChemPhysChem* **2011**, *12*, 1334–1341. [[CrossRef](#)] [[PubMed](#)]
23. Azar, H.A.; Hansen, C.T.; Costa, J. N:NIH(S)II-Nu/Nu Mice With Combined Immunodeficiency: A New Model for Human Tumor Heterotransplantation. *J. Natl. Cancer Inst.* **1980**, *65*, 421–430. [[CrossRef](#)] [[PubMed](#)]
24. Carlsson, G.; Gullberg, B.; Hafström, L. Estimation of Liver Tumor Volume Using Different Formulas-An Experimental Study in Rats. *J. Cancer Res. Clin. Oncol.* **1983**, *105*, 20–23. [[CrossRef](#)]
25. Elston, C.W.; Ellis, I.O. Pathological Prognostic Factors in Breast Cancer. I. The Value of Histological Grade in Breast Cancer: Experience from a Large Study with Long-Term Follow-Up. *Histopathology* **1991**, *19*, 403–410. [[CrossRef](#)] [[PubMed](#)]
26. Law, A.M.K.; Yin, J.X.M.; Castillo, L.; Young, A.I.J.; Piggitt, C.; Rogers, S.; Caldon, C.E.; Burgess, A.; Millar, E.K.A.; O'Toole, S.A.; et al. Andy's Algorithms: New Automated Digital Image Analysis Pipelines for FIJI. *Sci. Rep.* **2017**, *7*, 1–11. [[CrossRef](#)]
27. Ribatti, D.; Vacca, A.; Roncali, L.; Dammacco, F. The Chick Embryo Chorioallantoic Membrane as a Model for in Vivo Research on Anti-Angiogenesis. *Curr. Pharm. Biotechnol.* **2000**, *1*, 73–82. [[CrossRef](#)]
28. Carpentier, G.; Martinelli, M.; Courty, J.; Cascone, I. Angiogenesis Analyzer for ImageJ. In *4th ImageJ User and Developer Conference Proceedings*; Mondorf-les-Bains: Luxembourg, 2012; pp. 198–201.
29. Percie du Sert, N.; Hurst, V.; Ahluwalia, A.; Alam, S.; Avey, M.T.; Baker, M.; Browne, W.J.; Clark, A.; Cuthill, I.C.; Dirnagl, U.; et al. The ARRIVE Guidelines 2.0: Updated Guidelines for Reporting Animal Research. *PLoS Biol.* **2020**, *18*, e3000410. [[CrossRef](#)]
30. Sun, X.; Kaufman, P.D. Ki-67: More than a Proliferation Marker. *Chromosoma* **2018**, *127*, 175–186. [[CrossRef](#)] [[PubMed](#)]
31. Ribatti, D.; Nico, B.; Ruggieri, S.; Tamma, R.; Simone, G.; Mangia, A. Angiogenesis and Antiangiogenesis in Triple-Negative Breast Cancer. *Transl. Oncol.* **2016**, *9*, 453–457. [[CrossRef](#)] [[PubMed](#)]

32. Tabrizi, L.; Olasunkanmi, L.O.; Fadare, O.A. Experimental and Theoretical Investigations of Cyclometalated Ruthenium(II) Complex Containing CCC-Pincer and Anti-Inflammatory Drugs as Ligands: Synthesis, Characterization, Inhibition of Cyclooxygenase and in Vitro Cytotoxicity Activities in Various Can. *Dalt. Trans.* **2019**, *48*, 728–740. [[CrossRef](#)]
33. Navarro-Ranninger, C.; Zamora, F.; Masaguer, J.R.; Pérez, J.M.; González, V.M.; Alonso, C. Palladium(II) Compounds of Putrescine and Spermine. Synthesis, Characterization, and DNA-Binding and Antitumor Properties. *J. Inorg. Biochem.* **1993**, *52*, 37–49. [[CrossRef](#)]
34. Perše, M. Cisplatin Mouse Models: Treatment, Toxicity and Translatability. *Biomedicines* **2021**, *9*, 1406. [[CrossRef](#)] [[PubMed](#)]
35. Yamamoto, N.; Murata, K.; Fuke, H.; Inoue, T.; Yamanaka, Y.; Saitou, Y.; Ito, K.; Sugimoto, K.; Koyama, M.; Shiraki, K.; et al. Macrocytic Anemia during Low-Dose Cisplatin and 5-Fluorouracil through Implanted Infusion Port for Unresectable Hepatobiliary Malignancies. *Anticancer Res.* **2005**, *25*, 246.
36. Fei, L.; Huimei, H.; Dongmin, C. Pivalopril Improves Anti-Cancer Efficiency of CDDP in Breast Cancer through Inhibiting Proliferation, Angiogenesis and Metastasis. *Biochem. Biophys. Res. Commun.* **2020**, *533*, 853–860. [[CrossRef](#)] [[PubMed](#)]
37. Duyndam, M.C.A.; van Berkel, M.P.A.; Dorsman, J.C.; Rockx, D.A.P.; Pinedo, H.M.; Boven, E. Cisplatin and Doxorubicin Repress Vascular Endothelial Growth Factor Expression and Differentially Down-Regulate Hypoxia-Inducible Factor I Activity in Human Ovarian Cancer Cells. *Biochem. Pharmacol.* **2007**, *74*, 191–201. [[CrossRef](#)] [[PubMed](#)]
38. Aydinlik, S.; Uvez, A.; Kiyani, H.T.; Gurel-Gurevin, E.; Yilmaz, V.T.; Ulukaya, E.; Armutak, E.I. Palladium (II) Complex and Thalidomide Intercept Angiogenic Signaling via Targeting FAK/Src and Erk/Akt/PLC γ Dependent Autophagy Pathways in Human Umbilical Vein Endothelial Cells. *Microvasc. Res.* **2021**, *138*, 104229. [[CrossRef](#)] [[PubMed](#)]
39. Ulukaya, E.; Ari, F.; Dimas, K.; Ikitimur, E.I.; Guney, E.; Yilmaz, V.T. Anti-Cancer Activity of a Novel Palladium(II) Complex on Human Breast Cancer Cells in Vitro and in Vivo. *Eur. J. Med. Chem.* **2011**, *46*, 4957–4963. [[CrossRef](#)] [[PubMed](#)]
40. Ari, F.; Cevatemre, B.; Armutak, E.I.I.; Aztopal, N.; Yilmaz, V.T.; Ulukaya, E. Apoptosis-Inducing Effect of a Palladium(II) Saccharinate Complex of Terpyridine on Human Breast Cancer Cells in Vitro and in Vivo. *Bioorg. Med. Chem.* **2014**, *22*, 4948–4954. [[CrossRef](#)] [[PubMed](#)]